NANO LETTERS

2006
Vol. 6, No. 2
248−251

Periodic Square-Like Gold Nanoparticle Arrays Templated by Self-Assembled 2D DNA Nanogrids on a Surface

Junping Zhang, Yan Liu, Yonggang Ke, and Hao Yan*

Department of Chemistry and Biochemistry & The Biodesign Institute, Arizona State University, Tempe, Arizona 85287

Received November 9, 2005; Revised Manuscript Received January 3, 2006

ABSTRACT

We report the use of a self-assembled two-dimensional (2D) DNA nanogrid as a template to organize 5-nm gold nanoparticles (Au NPs) into periodic square lattices. Each particle sits on only a single DNA tile. The center-to-center interparticle spacing between neighboring particles is controlled to be ∼38 nm. These evenly distributed Au NP arrangements with accurate control of interparticle spacing may find applications in nanoelectronic and nanophotonic devices.

The collective properties of nanoparticles (NP) depend critically on their interparticle spacings and hierarchical organizations. For example, optical waveguiding based on metallic NPs requires accurate control of the distance between particles to allow light to propagate along a defined path efficiently.[1] The top-down approach has been the most widely used method to arrange NPs at specific positions, but it is a quite tedious process.[2] The bottom-up self-assembly approach has the advantage of massive parallelism but its application in controlling well-defined patterns of nanoparticle assemblies is still limited.[3]

In recent years, programmable self-assembly of DNA tiling lattices has been shown to be an effective way to construct well-defined nano- to micrometer scale structures from simple DNA building blocks.[4] Self-assembled DNA nanostructures offer programmable scaffolds to organize nanomaterials. For example, Au NPs conjugated with single-stranded DNA molecules have been used to assemble multimeric or chain-like structures through sequence-specific DNA hybridization.[5] Recently, Kiehl and co-workers[5c] have demonstrated the first use of self-assembled 2D DNA lattices to organize Au NPs into periodic striped patterns. In that work, 6-nm Au NPs conjugated with multiple T_{15} sequences were assembled into closely packed rows by in situ DNA hybridization to a preassembled 2D DNA scaffolding on a surface with a precisely defined interrow spacing of ∼63 nm. The intrarow particle spacing was less well controlled, ranging from 15 to 25 nm (center-to-center) as evidenced by TEM imaging.[5c] The explanation of this was that the diameter of the particles is larger than the intrarow spacing (∼4 nm) between the hybridization sites on the DNA lattice so that each multiply functionalized Au NP might connect to more than one hybridization site on the array. To achieve positioning of a single nanocomponent at a single hybridization site, larger spacings are required between the hybridization sites on the DNA array.

Here we report an effort to generate Au NP arrays of periodic square-like configurations on self-assembled DNA nanogrids. The square arrangement of NPs is particularly useful for constructing logic cellular nonlinear networks.[6] In contrast to the work reported previously,[5c] the larger spacing between neighboring tiles in the DNA lattice used here allowed us to assemble the NP arrays so that cross-hybridization between multiple sites is not possible. We also show an interesting finding that the layer of the DNA strands outside of the Au NPs plays a critical role that affects the interparticle spacings on the DNA nanogrid templates.

Figure 1 illustrates the design strategy and the DNA nanogrid structure. In this work, we utilize a family of DNA tiles that resemble a cross structure composed of four four-arm DNA branch junctions to template the assembly of Au NPs. A single unit of the cross structure has been shown to self-assemble into 2D nanogrids that display periodic square cavities.[4d] A two-tile system[4e] (tiles A and B) has also been developed such that tiles A and B associate with each other alternatively to form 2D nanogrids. Here we utilize the AB tile system and modified tile A so that each contains a short single-stranded DNA oligos of an A_{15} base sequence protruding out of the tile surface. This A_{15} sequence serves as the hybridization site to organize a 5-nm gold NP functionalized with a layer of T_{15} sequences. We have adopted a strategy reported previously[5c] to first self-assemble the 2D DNA nanogrids in solution and then deposit them

* Corresponding author. E-mail: hao.yan@asu.edu.

10.1021/nl052210l CCC: $33.50
Published on Web 01/17/2006

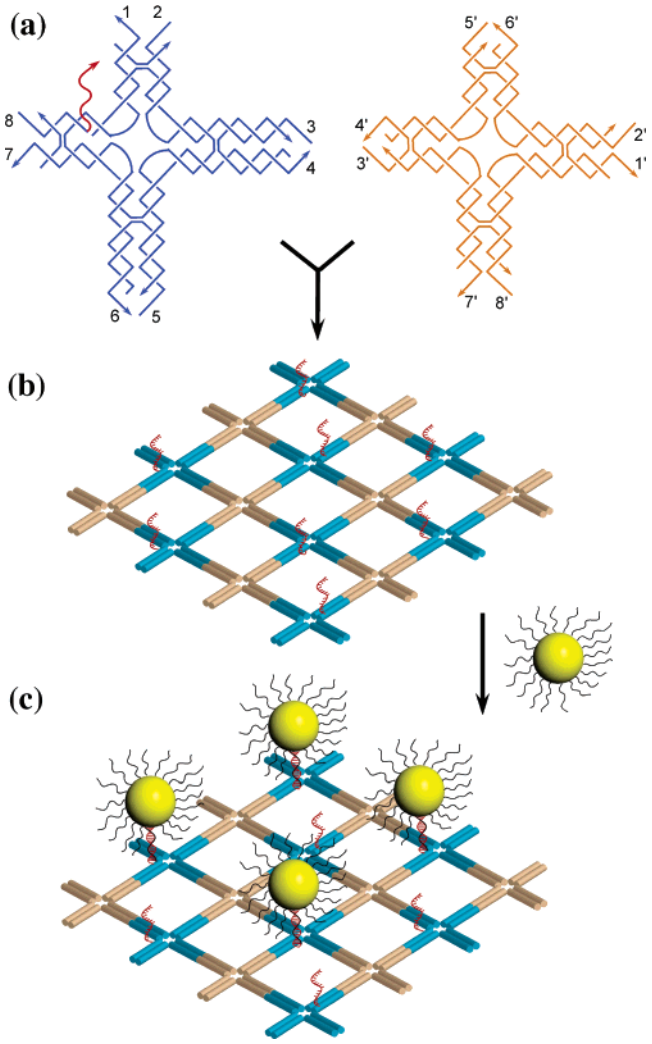

Figure 1. (a) Two-tile system to form the 2D DNA nanogrids. Tile A is blue, and tile B is orange. The numbers indicate the complementary sticky ends, with 1 pairing with 1′ and so on. The red strand on tile A is the A_{15} sequence. (b) The 2D DNA nanogrids with the single strand A_{15} on each A tile pointing out of the plane. (c) Assembly of 5-nm Au NPs on the DNA grids. The zigzag black lines surrounding the Au NPs represent the T_{15} strands covalently linked to the surface of the particle through Au−S bonds. Note that not all hybridization sites are attached with a Au NP; this is explained in Figure 2 and the main text.

on a mica surface. The Au NPs containing a layer of multiple T_{15} were then added onto the surface to allow the Au NPs to bind the hybridization sites on the DNA nanogrids. In Figure 1b, the distance between neighboring A and B tiles is 4 or 4.5 helical turns of DNA and the dimension of the cavities from center to center measure alternatively ∼17.6 or ∼19.3 nm. The distances between two neighboring hybridization sites are 25−27 nm in the diagonal direction and 35−39 nm in the linear direction.

Figure 2 shows atomic force microscopy (AFM) images and cross-section profiles demonstrating the in situ self-assembly of the Au NPs onto the DNA nanogrids. The AFM images and 3D surface plots in Figure 2a and b indicate the organization of the 5-nm Au NPs into periodic arrays with a square configuration. In Figure 2a, both the Au NPs and their underlying DNA nanogrids are visible. More AFM images of the NP arrays can be found in the Supporting Information. From the cross-section profile measurements (Figure 2c and d), the distance between neighboring Au NPs were measured to be ∼38 ± 1 nm. It appears that there is one Au NP missing at the center of each square containing 9 DNA tiles as illustrated in Figure 2e.

This observation that the NPs are missing regularly on the DNA nangrid template, at a first sight, is unexpected. We propose that the missing particle is a consequence of the dense layer of T_{15} on the outside of the Au NPs that not only increases the diameter of the particle, but also makes the Au NP surface highly negatively charged. Therefore, the Au NPs experience strong electric repulsion forces from the nearby particles when they were too close to each other. It has been shown before that even without a DNA layer at the outside, Au NPs like to form a close-packed lattice with a short gap between adjacent particles.[7] In our case, the minimum interparticle distance should be the largest of the following three lengths: the diameter of the particles including the ligands on the surface, the minimum distance between hybridization sites, and the location of the minimum potential energy as a function of interparticle distance. In this design, the effective diameter of the Au NPs containing a stretched single layer of T_{15} DNA strands[8] is ∼20 nm. The two smallest distances between the hybridization sites shown in Figure 2e are 25−27 nm (blue-to-blue-tile diagonal repeat) and 38 nm (blue-to-blue linear repeat). If every site had a Au NP, the edge-to-edge interparticle spacing would be 5−7 nm. If the middle tiles missed the Au NPs, the edge-to-edge spacing between the particles increases threefold to ∼18 nm. It is possible that if the particles occupy all of the hybridization sites, then they may experience too high an electric repulsion force from the nearby particles to stay stable. When the middle positions are avoided, the interparticle repulsion forces decrease to a point that the attraction forces from the T−A base pairing at the hybridization sites dominate.

This argument is supported by an image in Figure 3 showing the presence of local domains that particles attach to one of the two possible subregions (marked by blue and green dots, respectively). Both subregions contain a square arrangement of particles with many positions missing a particle. On the top half of the area shown, blue dots are mostly filled and all of the green dots are missing, whereas in the bottom half of the area shown, most of the green dots are filled and all of the blue dots are missing. In the center, a blue dot appears surrounded by three green dots. Thus, a particle is missing at the green dot in the right upper corner of that local square. This phenomenon can only be explained by the electric repulsion and not by steric hindrance because it appears from the AFM images that spatially a Au NP can fit in the cavity of a square of four particles. In any unit of a square of nine tiles cornered with the blue tiles, it is not possible to have all five blue tiles occupied with the Au NPs. Also, in any unit of a square of nine tiles cornered with the orange tiles, it is not possible to have all four blue tiles occupied with the Au NPs.

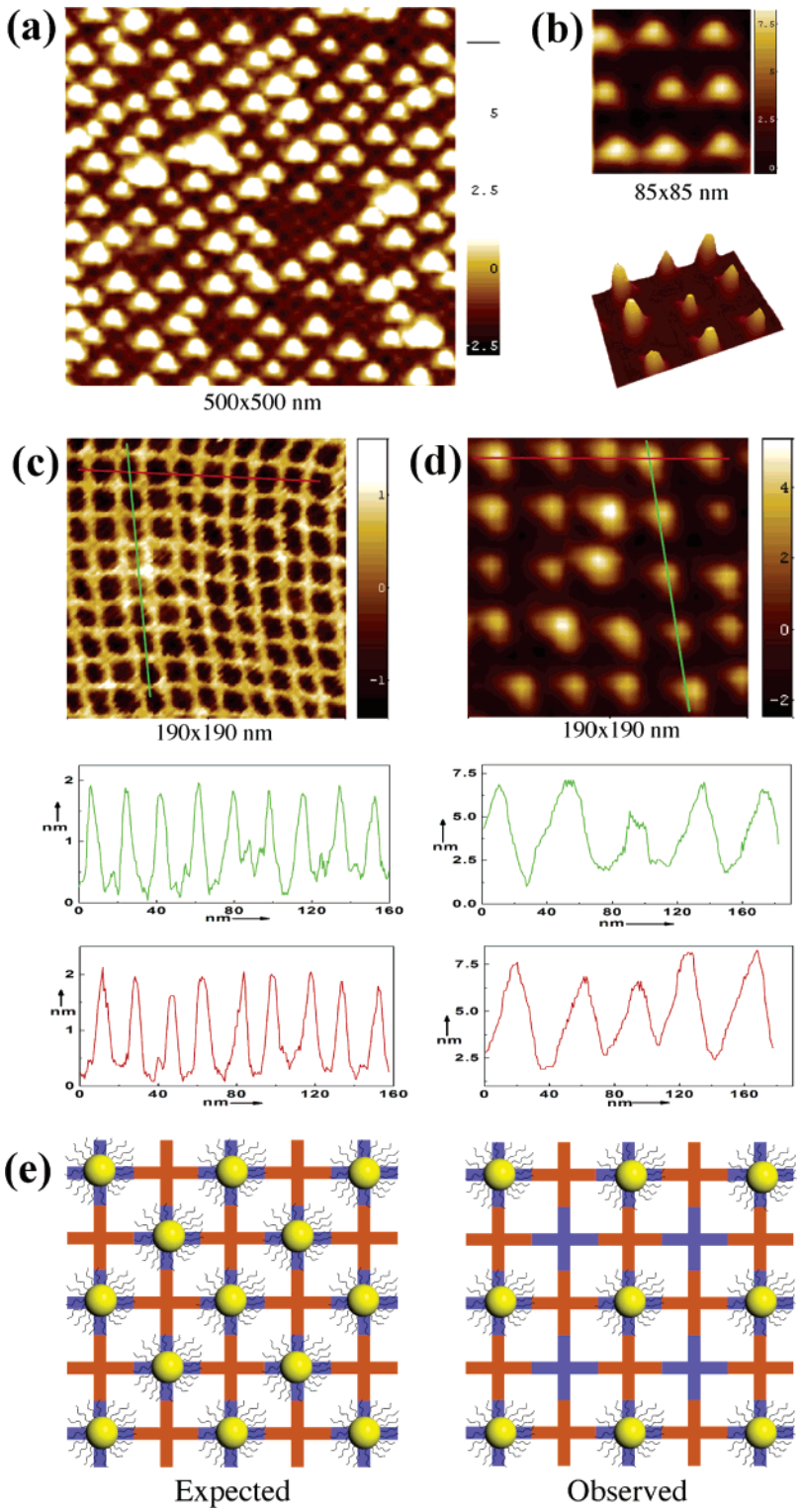

Figure 2. (a) AFM height image of the Au NPs assembled on the 2D DNA grids. (b) A zoom-in area showing the square configuration of the Au NP arrangements. A 3D view is also shown. Parts c and d compare the AFM images before and after gold NPs were assembled onto the DNA nanogrids. The profiles below the two images represent the cross-section profiles along the green and red lines in the images, respectively. (e) Schematic drawing of the assembly representing the scenarios if all sites are occupied and the observed case. The expected distances are 25−27 nm (blue-to-blue-tile diagonal repeat) and 38 nm (blue-to-blue linear repeat).

It should be pointed out that in the work of Kiehl and co-workers,[5c] using the same strategy for the assembly of Au NPs on double crossover DNA arrays, the center-to-center interparticle spacings in the periodic square lattices range from 15 to 25 nm. In their work, the spacing between the hybridization site is ∼4 nm. Therefore, for any single Au NP, it could hybridize with multiple neighboring tiles in the same row so that the attraction force holding a Au NP

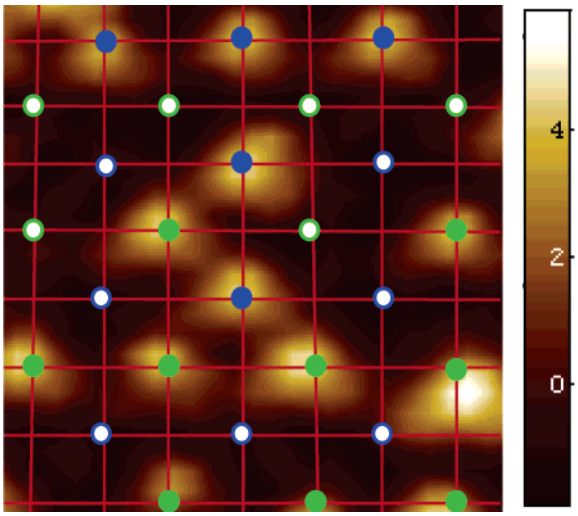

Figure 3. Scenario of a domain shift arrangement of Au NPs on the DNA lattice. Schematic grid lines (red lines) and Au NPs are superimposed on the AFM image to illustrate such a domain shift. The position of each Au NP can be assigned by one of the two possible hybridization sites, as marked by blue and green dots. Solid dots represent filled sites, and white color filled dots represent missing sites. Scale: 130 × 130 nm^2.

in position is much stronger than the force with a single hybridization in our case; thus, a smaller interparticle distance was allowed.

In summary, we have used a self-assembled 2D DNA nanogrid successfully as template to organize 5-nm Au NPs into square lattice. The center-to-center interparticle spacing between neighboring particles is controlled to be ∼38 nm. Each particle sits on only a single DNA tile. Kiehl and co-workers[9] demonstrated recently that the in-situ Au NP assembly strategy can be extended to organize different-sized Au NPs each encoded with a unique DNA sequence. Therefore, it is possible to self-assemble more complex nanoparticle patterns using addressable DNA nanogrids.[10] This could allow us to self-assemble nanoparticle constructs that may lead to applications in nanoelectronic and nanophotonic devices.

Acknowledgment. We thank Professor Richard Kiehl and Dr. Yariv Pinto at University of Minnesota for helpful discussions. We also thank Professor Stuart Lindsay at Arizona State University for proofreading the manuscript. This work has been supported by grants from the NSF to H.Y. and grant from Arizona State University.

Supporting Information Available: DNA sequences, experimental methods, and additional AFM images. This material is available free of charge via the Internet at http://pubs.acs.org.

References

(1) Maier, S. A.; Brongersma, A. L.; Kik, P. G.; Atwater, H. A. *Phys. Rev. B.* **2002**, *65*, 193408.
(2) Wang, D. Y.; Mohwald, H. *J. Mater. Chem.* **2004**, *14*, 459−468.
(3) Andres, R. P. et al. *Science* **1996**, *273*, 1690−1693.
(4) (a) Winfree, E.; Liu, F.; Wenzler, L. A.; Seeman, N. C. *Nature* **1998**, *394*, 539−544. (b) LaBean, T. H.; Yan, H.; Kopatsch, J.; Liu, F.; Winfree, E.; Reif, J. H.; Seeman, N. C. *J. Am. Chem. Soc.* **2000**, *122*, 1848−1860. (c) Mao, C.; Sun, W.; Seeman, N. C. *J. Am. Chem. Soc.* **1999**, *121*, 5437−5443. (d) Yan, H.; Park, S. H.; Finkelstein, G.; Reif, J. H.; LaBean, T. H. *Science* **2003**, *301*, 1882−1884. (e) Park, S. H.; Yin, P.; Liu, Y.; Reif, J. H.; LaBean, T. H.; Yan, H. *Nano Lett.* **2005**, 5, 729−733. (f) Liu, D.; Wang, M.; Deng, Z.; Walulu, R.; Mao, C. *J. Am. Chem. Soc*. **2004**, *126*, 2324−2325. (g) Ding, B.; Sha, R.; Seeman, N. C. *J. Am. Chem. Soc.* **2004**, *126*, 10230−10231. (h) Rothemund, P. W. K.; Papadakis, N.; Winfree, E. *PLoS Biol.* **2004**, *2*, 2041−2053. (i) Malo, J.; Mitchell, J. C.; Vénien-Bryan, C.; Harris, J. R.; Wille, H.; Sherratt, D. J.; Tuberfield, A. J. *Angew. Chem., Int. Ed.* **2005**, *44*, 3057−3061. (j) Chelyapov, N.; Brun, Y; Gopalkrishnan, M.; Reishus, D.; Shaw, B.; Adleman, L. *J. Am. Chem. Soc.* **2004**, *126*, 13924−13925.
(5) (a) Loweth, C. J.; Caldwell, W. B.; Peng, X.; Alivisatos, A. P.; Schultz, P. G. *Angew. Chem., Int. Ed.* **1999**, *38*, 1808−1812. (b) Xiao, S.; Liu, F.; Rosen, A. E.; Hainfeld, J. F.; Seeman, N. C.; Musier-Forsyth, K.; Kiehl, R. A. *J. Nanopart. Res.* **2002**, *4*, 313. (c) Le, J. D.; Pinto, Y.; Seeman, N. C.; Musier-Forsyth, K.; Taton, T. A.; Kiehl, R. A. *Nano. Lett.* **2004**, 4, 2343. (d) Deng, Z.; Tian, Y.; Lee, S.; Ribbe, A. E.; Mao, C. *Angew. Chem., Int. Ed.* **2005**, *44*, 3582−3585. (e) Claridge, S. A.; Goh, S. L.; Fréchet, J. M. J.; Williams, S. C.; Micheel, C. M.; Alivisatos, A. P. *Chem. Mater.* **2005**, *17*, 1628−1635.
(6) Yang, T.; Kiehl, R. A.; Chua, L. O. *Int. J. Bifurcation Chaos Appl. Sci. Eng.* **2001**, *11*, 2895−2912.
(7) Kim, B.; Tripp, S. L.; Wei, A. *J. Am. Chem. Soc.* **2001**, *123*, 7955−7956.
(8) Parak, W. J.; Pellegrino, T.; Micheel, C. M.; Gerion, D.; Williams, S. C.; Alivisatos, A. P. *Nano Lett.* **2003**, *3*, 33−36.
(9) Pinto, Y.; Le, J. D.; Seeman, N. C.; Musier-Forsyth, K.; Taton, T. A.; Kiehl, R. A. *Nano Lett.* **2005**, *5*, 2399−2402.
(10) Lund, K.; Liu, Y.; Lindsay, S.; Yan, H. *J. Am. Chem. Soc.* **2005**, *127*, 17606−17607.

NL052210L